International Immunopharmacology 96 (2021) 107658

Contents lists available at ScienceDirect

International Immunopharmacology

journal homepage: www.elsevier.com/locate/intimp

A natural product, Piperlongumine (PL), increases tumor cells sensitivity to NK cell killing

Lukman O. Afolabi [a,c,1], Jiacheng Bi [a,b,c,1], Liang Chen [a,c], Xiaochun Wan [a,c,*]

[a] Guangdong Immune Cell Therapy Engineering and Technology Research Center, Center for Protein and Cell-based Drugs, Institute of Biomedicine and Biotechnology, Shenzhen Institutes of Advanced Technology, Chinese Academy of Sciences, Shenzhen 518055, PR China
[b] CAS Key Laboratory of Quantitative Engineering Biology, Shenzhen Institute of Synthetic Biology, Shenzhen Institutes of Advanced Technology, Chinese Academy of Sciences, Shenzhen 518055, PR China
[c] University of Chinese Academy of Sciences, Beijing 100864, PR China

ARTICLE INFO

Keywords:
Cancer
Natural Killer cell
Piperlongumine
Immunomodulators
Cytotoxicity

ABSTRACT

Natural Killer (NK) cells are components of innate immune surveillance against transformed cells. NK cell immunotherapy has attracted attention as a promising strategy for cancer treatment, whose antitumor effects, however, require further improvement. The use of small molecules with immunomodulatory potentials and selective tumor-killing possesses the potential to complement immunotherapy. This study demonstrated that Piperlongumine (PL), a natural alkaloid obtained from long pepper fruit, alone has antitumor and anti-proliferative potential on all the tested tumors in vitro. PL pretreatment of tumor cells also potentiates their susceptibility to NK cell cytolysis at the doses where NK cell functions were preserved. Importantly, PL suppresses both NK –sensitive MHC-I –deficient and MHC-I –sufficient tumor growth in vivo. Mechanistically, PL induces misfolded proteins, impedes autophagy, increases ROS and tumor conjugation with NK cells. Furthermore, PL enhances the expression of NK cell-activating receptors on NK cells and its ligands on tumor cells, possibly leading to increased susceptibility to NK cell killing. Our findings showed the antitumor and immunomodulatory potential of PL, which could be explored to complement NK cell immunotherapy for cancer treatment.

1. Introduction

NK cells are the first line of host immune surveillance [1]. They play critical antitumor and anti-viral roles on stressed or transformed cells through direct cytotoxicity or by secretion of cytokines/chemokines [1,2]. The use of NK cell cancer immunotherapy as a viable treatment option has been well discussed [3,4]. However, NK cells in the tumor microenvironment are usually functionally compromised, requiring additional stimulation of their activity or combinations with other antitumor strategies [5,6]. The induction of stress in tumor cells by small molecules can lead to the release of stress molecules such as damage-associated molecular patterns (DAMPs), which can trigger immune effector cells [7]. Additionally, drug-induced stress pathways can alter the expression pattern of NK cell-activating and inhibitory ligands on tumor cells, rending them sensitive to NK cell cytolysis [8].

Small molecules are capable of eliciting antitumor activity while simultaneously serving as an immunomodulatory agent. Piperlongumine (PL) is a natural alkaloid obtained from long pepper fruit *Piper longum*. As a small molecule, PL's chemical structure has been well characterized (Fig. 1A) [9]. Reports have shown that PL exhibits promising antitumor potentials and can exert a broad spectrum of biological effects in tumor cells [10,11]. PL's ability to evoke cell cycle arrest, autophagy, DNA damage, inhibition of angiogenesis, and cell proliferation, among others [12–14], suggests it is a promising molecule that can be exploited for cancer therapy. Several studies have also shown the selective killing of tumor cells by PL treatment and not on normal cells [9,15]. The associated mechanism of tumor-specific killing of PL includes binding to ROS defensive proteins such as carbonyl reductase 1 (CBR1) or glutathione S-transferase Pi 1 (GSTP1); hence, rendering tumor cells unable to cope with increasing ROS generation [9,13].

* Corresponding author at: Guangdong Immune Cell Therapy Engineering and Technology Research Center, Center for Protein and Cell-based Drugs, Institute of Biomedicine and Biotechnology, Shenzhen Institutes of Advanced Technology, Chinese Academy of Sciences, Shenzhen 518055, PR China.
E-mail address: xc.wan@siat.ac.cn (X. Wan).
[1] These authors have contributed equally to this work.

https://doi.org/10.1016/j.intimp.2021.107658
Received 15 December 2020; Received in revised form 8 March 2021; Accepted 3 April 2021
Available online 19 April 2021

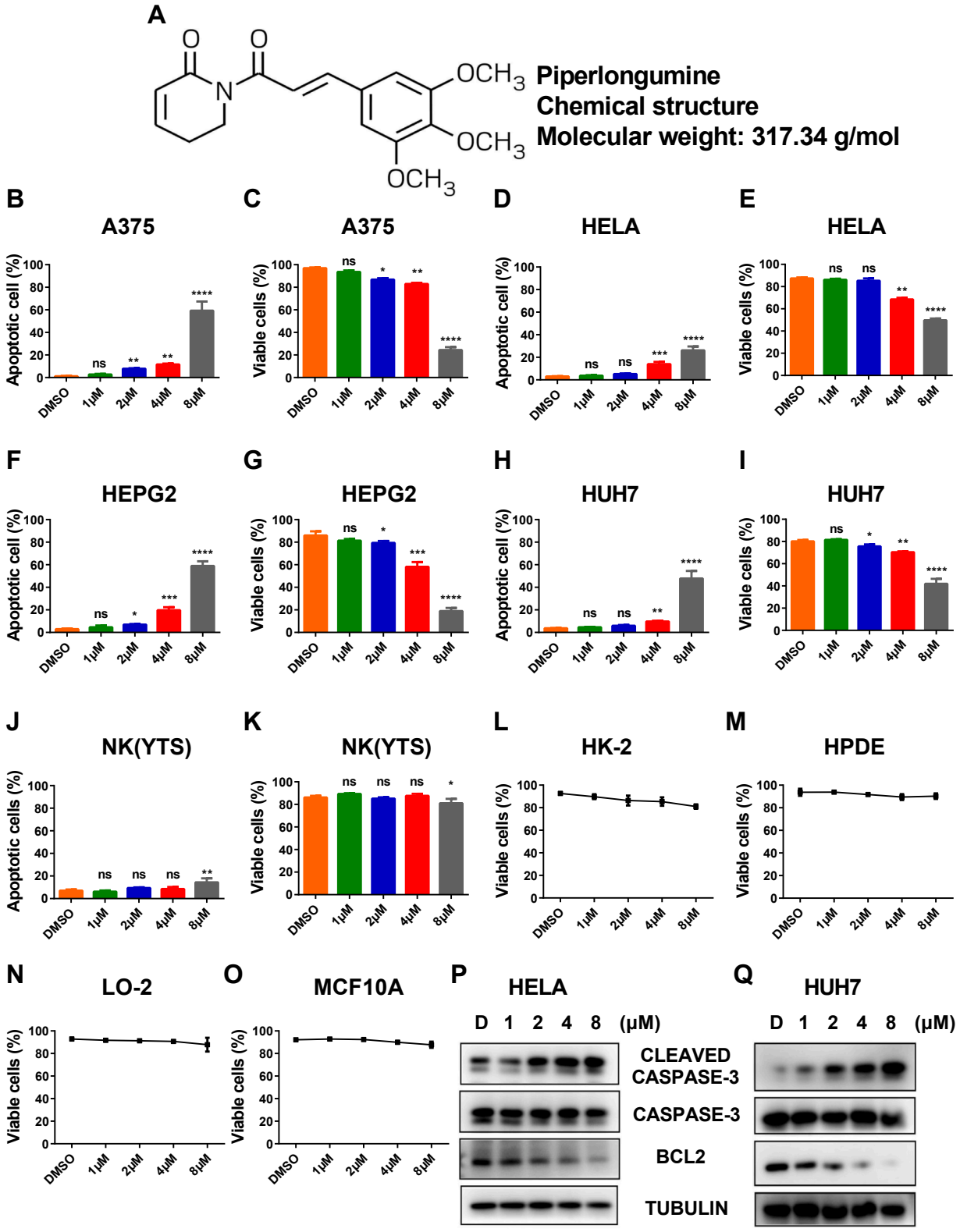

Fig. 1. Piperlongumine (PL) displayed potent tumorigenic activity in a dose-dependent manner but did not affect normal human cell lines cell viability. Piperlongumine (PL) treatment on tumor cell viability. (A) Molecular Structure of Piperlongumine; (B, D, F, H) apoptotic cells; (C, E, G, I) viable tumor cells after 24 hours of increasing dose (1–8 μM) of Piperlongumine (PL) treatment with DMSO controls. (B, C) human skin cell carcinoma A375, (D, E) human cervical carcinoma HELA, (F, G) human hepatocellular carcinoma HEPG2, (H, I) human hepatocarcinoma HUH7. Assessment of in vitro PL treatment on NK (YTS) and normal human cell line viability. (J, K) clonal human NK cell line, (L) Human Kidney cell line (M) Human Pancreatic Duct Epithelial Cell Line, (N) Human Hepatic Cell Line, and (O) Human Mammary Epithelial Cells. (P, Q) Western-blot analysis for apoptosis-related proteins after 24 h treatment of increasing dose (1–8 μM) of PL on tumor cells. (P) HELA, (Q) HUH7. Data represent mean ± SD (n ≥ 3 replicates) from three independent experiments (B–K). (not significant ns, $P > 0.05$, *$P \leq 0.05$, **$P \leq 0.01$, ***$P \leq 0.001$, ****$P \leq 0.0001$) assessed by unpaired *t*-test.

Besides, PL can also decrease thioredoxin reductase 1 (TrxR1) activity, a vital antioxidant system that plays a critical role in regulating cellular redox processes, thereby elevating ROS level [16].

While many studies have demonstrated the antitumor potentials of PL, reports on its immunomodulatory roles remain elusive. In the current study, we focused on evaluating the antitumor and immunomodulatory functions of PL on selected tumor cell lines.

2. Materials and methods

2.1. Cell lines and culture

The A375, Hela, HepG2, and Huh7 cell lines used in this study were obtained from ATCC, while NK (YTS) cell line (clonal human NK cell line) and RMA-S (MHC-I –deficient) were preserved in-house. HPDE, LO-2, HK-2, and MCF10A cell lines were used as control normal cells. The A375, Hela, HepG2, Huh7, LO-2, HK-2, and MCF10A cell lines were cultured in DMEM medium, HPDE was grown in DMEM/F12 + endothelial growth factor (EGF), while YTS and RMA-S cell line were grown in RPMI-1640 (Corning) medium. All media were supplemented with 10% heat-inactivated fetal bovine serum (FBS), 100 U/ml of penicillin, and 100 μg/ml of streptomycin (Gibco-BRL, Gaithersburg, MD), 2 mM L-glutamine, and cells were incubated at 37 °C with 5% CO2 as described [17,18].

2.1.1. Drugs, reagents, and antibodies

Piperlongumine (Cat. No.: HY-N2329) was obtained from MedChemExpress (Shanghai, China) and was made up of a stock solution of 10 mM in DMSO (Sigma-Aldrich, D2650), N-Acetyl-L-cysteine (Sigma-Aldrich, A9165), Bromhexine hydrochloride (MedChemExpress, HY-B0372A), cOmplete™ Protease Inhibitor Cocktail (Roche Diagnostics 04693116001), Anti-Poly-ubiquitin (Abcam ab190061, 1:5000), LC3B (Abcam ab51520, 1:3000), GAPDH (Santa Cruz Biotech sc-47724, 1:2000), α Tubulin (B-7) (Santa Cruz sc-5286, 1:2000), BCL2 (Proteintech, 60178-1-Ig), Caspase-3 (CST 9662), Cleaved Caspase-3 (Asp175) (CST 9661), Secondary antibodies conjugated to HRP: Anti-rabbit (CST 7074), Anti-mouse (Santa Cruz Biotech sc-2357). InVivoMAb anti-mouse NK1.1 (clone PK136. BioXCell BE0036-5), InVivoMAb Mouse IgG2a, κ (clone C1.18.4, BioXCell BE0085).

Antibodies for flow cytometry: (anti mouse antibodies were used and all from BioLegend unless otherwise indicated): FITC-CD3ε (145-2C11), BV-510 -CD45 (103138), APC-NK-1.1 (Clone PK136) (108710), BV-510 -NK-1.1 (Clone PK136) (108737), PE-CD69 (104507), PE-CD107A (121612), PE-NKG2D (115606). Anti-human antibodies used were: APC-CD56 (362504), APC-CD28 (983406), APC-CD226 (338311), PE Fas-L (306406), BV LFA-1 (363407), PE-NKG2D (320806), APC-NKp46 (331917), APC-CD80 (305219), APC-CD86 (374207), PE-CD112 (337410). Isotype control antibodies: APC-Rat IgG1 (401904), PE-Rat IgG1 (401906), BV-Rat IgG1 (401911).

2.2. Apoptosis detection

Cell apoptosis was evaluated using Pacific Blue™ Annexin V Apoptosis − 7-aminoactinomycin D (7-AAD) Detection Kit (640926, BioLegend, San Diego, CA). The assay was performed as recommended by the manufacturer. The analysis was done by flow cytometry, excluding cellular debris.

2.3. Real-time in vitro proliferation assay

The cellular response of A375, Hela, HepG2, and Huh7 cell lines to Piperlongumine (PL) treatment was assessed by the xCELLigence RTCA (ACEA Biosciences Inc.) as previously described [19–21]. Briefly, 10^4 cell/50 μl (per well) were seeded into the 96X E-Plates and monitored until a log growth monolayer was obtained (approximately 18–24 h). Increasing doses of PL (1, 2, 4, 8 μM) or DMSO control were added into each well to make 200 μl complete media. The SP station of the RTCA was allowed to continuously measure the Cell Index (CI) every 15 min for ≥ 70 h (or indicated time) of incubation. CI was normalized at the end of the experiment to remove any well-well variation.

2.3.1. In vitro NK (YTS) cell cytolysis

NK cell cytotoxicity against PL pretreated tumor cells was performed using the x-CELLigence real-time cell analysis (RTCA SP) described previously [19]. In brief, 2 μM of PL or DMSO was used to pretreat target tumor cells (A375, Hela, HepG2, and Huh7) for 20 h, and media was changed to complete media. NK (YTS) cells were added directly to the pretreated cells at different effector: target ratios (E: T). Background controls were done by seeding target cells without adding effector cells. The Cell Index (CI) was measured continuously for the indicated number of hours after effector cell addition. CI was normalized at the end of the experiment to remove any well-well variation using the RTCA software Pro (version 2.3.0). Percentage cytolysis was calculated at the end of the experiment as:

$$\% \text{ Cytolysis} = ((CI_{\text{no effector}} - CI_{\text{effector}}) / (CI_{\text{no effector}})) \times 100$$

For the co-treatment experiment, PL and NK cells were added to the target cells together. These reagents were added together with PL onto the target cells for the experiment involving N-acetyl-L-cysteine (NAC) and Bromhexine hydrochloride (BRH).

All experiments were performed in three independent experiments with four or more replicates at various effector-to-target (E: T) ratios.

2.4. Misfolded protein clearance assay:

The level of K-48 polyubiquitinated proteins was assayed as described by [22,23]. Briefly, cells were treated with increasing doses of Piperlongumine (1, 2, 4, 8 μM) or DMSO control for 24 h. The cells were harvested and lysed with a non-ionic detergent (NP-40) buffer for 30 mins on ice; the whole lysate was centrifuged at 12,000 g for 15 min at 4 °C. The NP-40-soluble supernatant was marked NS fraction, transferred to a new tube, and the protein lysate was quantified by Bradford assay (Bio-Rad Labs). The insoluble pellet was resuspended in 2% SDS with 50 mM DTT (SDS buffer). This fraction is labeled SDS soluble (SS) fraction. Both the NP-40-soluble (NS) and SDS soluble (SS) portions were heated at 98 °C for 8 min in Laemmli sample buffer and resolved by SDS-PAGE and protein transferred onto PVDF membranes followed by immunoblotting.

Primary antibodies specific to K48 polyubiquitin proteins (Abcam ab190061) and secondary antibodies conjugated to HRP: Anti-rabbit (CST 7074) were used. The immunoblots were developed using ECL reagents and viewed using Amersham Imager 680.

2.4.1. Detection of LC3 by western blot

Cells were treated with 2μM of Piperlongumine and harvested at the specified time points (4, 8, 12, and 24hrs), with the corresponding untreated control cells. The cells were washed with PBS and lysed with RIPA (50 mM Tris pH 8.0, 150 mM NaCl, 1% NP-40, 0.5% sodium deoxycholate, 0.1% SDS) supplemented with protease inhibitor cocktail (PIC) for 30 mins on ice. The lysate's total protein content was quantified and heated at 98 °C for 8 min in Laemmli sample buffer and resolved by SDS-PAGE. The proteins were transferred onto PVDF membranes, followed by immunoblotting. LC3B specific primary antibodies and HRP conjugated secondary antibodies were used, followed by the development of the immunoblots using ECL reagents and viewed using Amersham Imager 680.

2.5. Reactive oxygen species (ROS) measurement

Total cellular ROS was measured using Cellular Reactive Oxygen Species Detection Assay Kit (Deep Red Fluorescence, Abcam -ab186029). The assay was performed as recommended by the manufacturer. Cells were treated with increasing doses of Piperlongumine

(PL) (1, 2, 4, 8 μM) or DMSO control. The cells were harvested and then incubated with the ROS reagents for 30 min, at 37 °C and 5% CO2, and immediately analyzed by flow cytometry. The respective signals were analyzed by CytoFLEX LX Flow Cytometer (Beckman Coulter).

2.6. NK–target cell conjugation assay

Conjugation of the NK (YTS) cell and the target (A375, Hela, HepG2, and Huh7) cells was performed as described [24]. Briefly, target cells were exposed to 2 μM of Piperlongumine for 24 hours, harvested, and washed with PBS to remove the drug. The target cells were stained with CFSE, while NK (YTS) cells were stained with anti-human CD56-APC antibody (362504, BioLegend). The stained cells were co-incubated at 37 °C for the indicated time at a 1:2 effector-target ratio, followed by cell fixing using True-Nuclear™ Transcription Factor Buffer (BioLegend). The samples were analyzed by CytoFLEX LX Flow Cytometer (Beckman Coulter) and conjugates formed are indicated by double-positive signals for CFSE and CD56-APC.

2.7. Detection of surface receptors on NK(YTS) and tumor cells

To evaluate the effect of PL on the expression of receptors and ligands on NK (YTS) and tumor cells, the cells were pretreated with PL or DMSO control for 20 hours, washed twice with PBS, and resuspended in cell staining buffer. The cells were then stained with the specific fluorophore-conjugated antibodies or their respective IgG controls for 30 min at 4 °C, washed again, and then directly analyzed by FACS.

For In vivo analysis of splenic NK cells, spleen isolated from PL and untreated B16F10 tumor-bearing mice was homogenized through a 70-μm filter in PBS, a single-cell suspension was prepared from the splenocytes followed by treatment with ACK Lysis buffer to lyse the RBC as described [25]. Splenocytes were washed and resuspended in cell staining buffer. The cells were labeled with the specific fluorophore-conjugated anti-mouse antibodies. The data was acquired using CytoFLEX LX Flow Cytometer (Beckman Coulter) and analyzed using FlowJo software (version 7.6).

2.8. Mice

Six to eight-weeks old C57BL/6 and BALB/c mice were used. The experimental procedures and animal handling strictly followed the approved protocols and guidelines of the Shenzhen Institute of Advanced Technology, Chinese Academy of Sciences (CAS).

2.8.1. In vivo experiments

For the pretreatment experiment, RMA-S tumor cells were pretreated with 2 μM of Piperlongumine or DMSO (control) for 24 hours before inoculation with 1 X 10^6 cells/mice. To test PL therapy, C57BL/6 and BALB/c mice were subcutaneously injected with RMA-S (1 X 10^6 cells/mice), B16F10 (2 X 10^5 cells/mice), and CT26 (2x 10^5 cells/mice) cells, respectively. The mice were randomly distributed into two groups of six mice per group. Therapy commenced two days after tumor injection with 10 mg/kg/day Piperlongumine or PBS (untreated group) intraperitoneally (i. p). Tumor size and body weight were recorded every three days, and all mice were sacrificed when tumor volume reached 1500 mm^3.

2.8.2. NK cell depletion

To deplete $NK1.1^+$ cells, C57BL/6 were intraperitoneally administered with 200 μg mAb to NK1.1 (PK136) or Isotype control one day before tumor challenge. PL therapy commenced two days after the tumor challenge.

2.9. Statistical analysis

Data were analyzed with GraphPad Prism6 software using the unpaired two-tailed Student's *t*-test, two-way ANOVA.

3. Results

3.1. Piperlongumine (PL) induces apoptosis in tumor cells

To investigate the pro-apoptotic effect of PL on selected tumors (A375, Hela, HepG2, and Huh7) cell lines, increasing PL concentrations were exposed to cells for 24 hours. As little as 2 μM of PL initiated apoptosis in A375 cells (Fig. 1B), the percentage of apoptotic cells increased in a dose-dependent manner compared with DMSO control. However, only 4 μM or higher concentration of PL was sufficient to induce apoptosis in Hela cells (Fig. 1D), while PL had a similar response in HepG2 as seen for A375 cells (Fig. 1F). On the other hand, the induction of apoptosis in Huh7 cells requires 4–8 μM of PL treatment (Fig. 1H). An increasing percentage of apoptotic cells was observed for all PL-treated tumor cells in a dose-dependent manner, with 4–8 μM of PL sufficient to induce apoptosis in all tested cell lines.

Moreover, PL treatment significantly decreased tumor cell viability in a dose-dependent manner Fig. 1(C, E, G, and I) compared with vehicle-only treated controls. To further substantiate the observed induction of apoptosis by PL treatment, we assessed the possible mechanism through which PL induces apoptosis in these tumor cell lines. Two of these cell lines (Hela and Huh7) were treated with increasing dose (1–8 μM) of PL for 24 hours, and some apoptosis-related proteins were assessed by western blot. Immunoblotting of the pro-caspase-3 and cleaved caspase-3 (critical players in induction of cellular apoptosis) revealed that PL could induce these pro-apoptotic proteins' expression (Fig. 1P -Q). Additionally, an assessment of the Bcl family's anti-apoptotic protein in these cells showed that PL treatment could inhibit the anti-apoptotic function of Bcl-2 protein in a dose-dependent manner (Fig. 1P -Q). Therefore, PL is capable of inducing apoptosis in tumor cells, possibly through a caspase-dependent manner.

3.1.1. Piperlongumine (PL) preserved the viability and activity of natural killer (NK), and normal cell lines

We evaluated PL treatment's effect on four normal human cell lines (HPDE, LO-2, HK-2, MCF10a) and YTS viability after 24 hours of increasing doses of PL exposure. Fig. 1J and K showed concentrations below 8 μM failed to induce apoptosis nor affect YTS cell viability. Similarly, the viability of the four normal cell lines tested after PL treatment were preserved (Fig. 1L-O).

Based on this result, we investigated the immunomodulatory effects of PL at non-NK cell apoptotic concentrations.

3.2. Piperlongumine (PL) growth inhibitory activity in tumor cells

The real-time proliferation profiles obtained from the x-CELLigence (RTCA SP) system revealed a significant growth inhibitory effect of PL on all treated tumor cells in a dose-dependent manner compared to vehicle-only treated controls (Fig. 2A–D). The proliferation profiles at the end of the experiment showed a significant inhibitory effect on all tumor cells. A375, Hela, HepG2, and Huh7 cells showed more sensitivity to all the PL dosages than their respective controls (Fig. 2E–H). Therefore, PL could suppress the growth of tumor cells in vitro.

3.3. Piperlongumine (PL) pretreatment of tumor cells enhances their NK cells' cytotoxicity

To investigate PL's immunomodulatory effects, we pretreated tumor cells with PL before NK cell cytolysis (Fig. 3A–H). As shown in Fig. 3A and B, A375 tumor cells pretreated with PL had increased NK cell cytolysis compared to vehicle-treated only for the different E:T ratios. Similarly, PL pretreatment of Hela cells (Fig. 3C and D), HepG2 cell (Fig. 3E and F), and Huh7 cell (Fig. 3G and H) all displayed a significant increase in NK cell-mediated killing. This observation revealed that

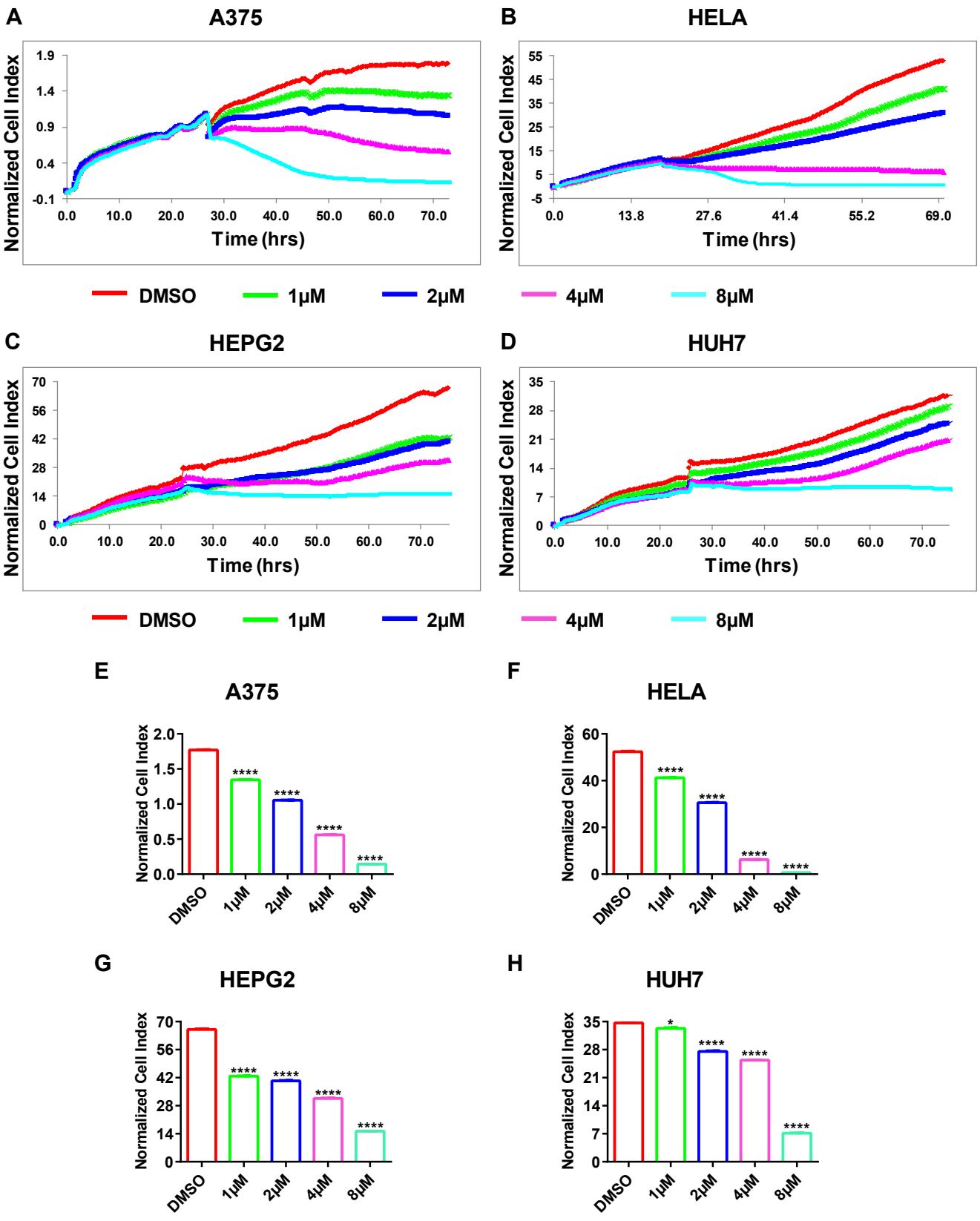

Fig. 2. Piperlongumine (PL) showed anti-proliferative activity on tumor cells. Proliferation profiles from the REAL-TIME Cell Analyzer (RTCA). Tumor cells were treated with increasing dose (1–8 μM) of PL and DMSO control for the specified number of hours. (A, E) human skin cell carcinoma A375, (B, F) human cervical carcinoma HELA, (C, G) human hepatocellular carcinoma HEPG2, (D, H) human hepatocarcinoma HUH7. Cell Index (CI)was normalized to remove any well-well variation; it indicates cell number, cell–cell attachment, cell size, etc. (Increase CI indicates cell growth). Data represent mean ± SD (n ≥ 3 replicates) from three independent experiments(E–H). (not significant ns, $P > 0.05$, *$P \leq 0.05$, ****$P \leq 0.0001$) assessed by unpaired *t*-test.

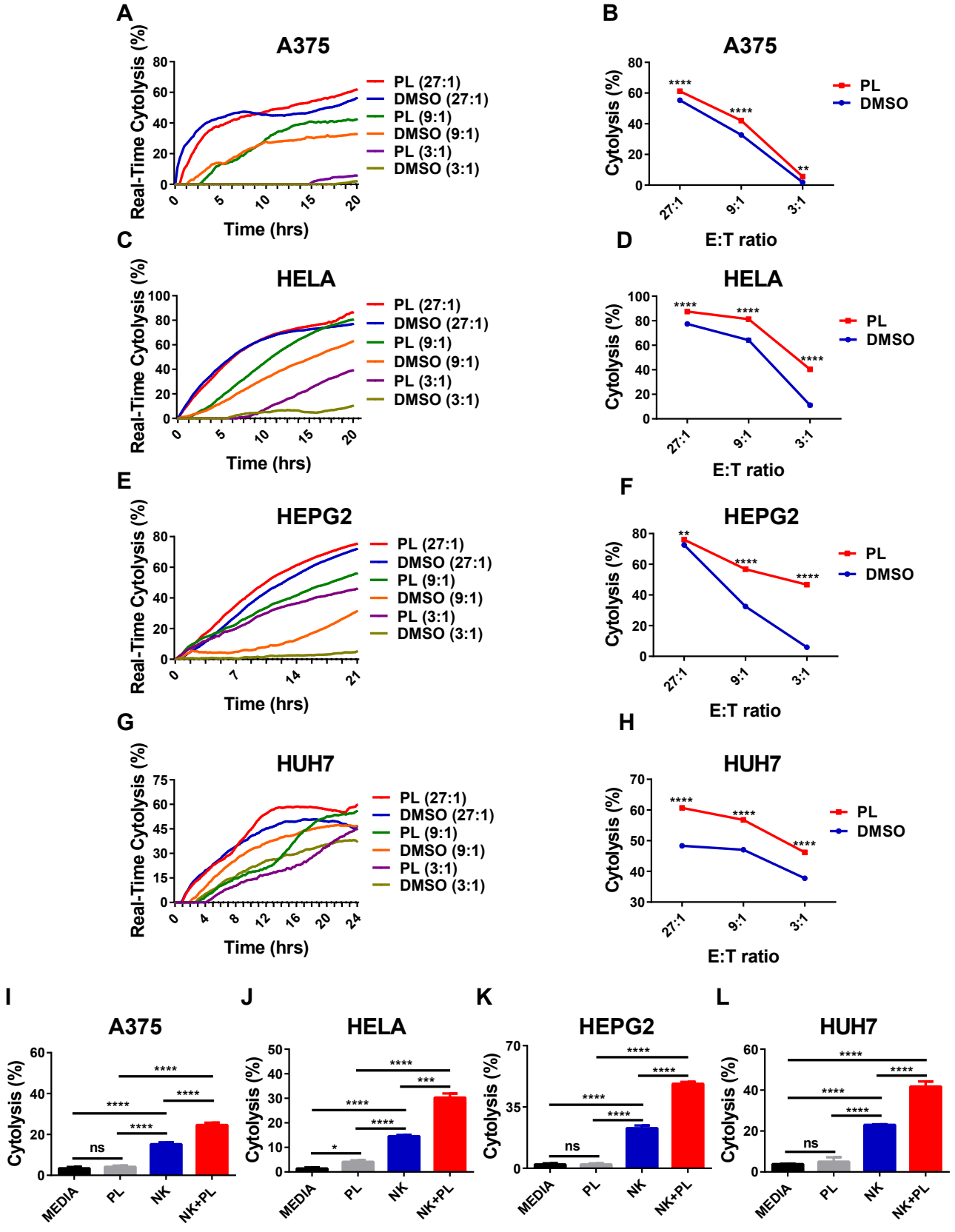

Fig. 3. Piperlongumine (PL) Pretreatment of Tumors increases their sensitivity to NK cell-mediated cytotoxicity. In vitro NK cell cytotoxicity of Piperlongumine (PL) pretreated tumor cells. The cells were pretreated with 2 μM of PL or DMSO control for 20 hours before NK cell cytolysis. (A, C, E, G) real-time NK cell cytolysis using the REAL-TIME Cell Analyzer (RTCA); (B, D, F, H) NK cell cytolysis of tumor cells at different E: T ratio. (A, B) A375, (C, D) HELA, (E, F) HEPG2, (G, H) HUH7. (I, J, K, L) In vitro evaluation of cytotoxicity of PL and NK cell co-treatment on the tumor cell lines. (I) A375, (J) HELA, (K) HEPG2, (L) HUH7. Percentage cytolysis is expressed as mean ± SD for each E: T ratio ($n \geq 4$ replicates) from three independent experiments (B, D, F, H, I, J, K, L). (not significant ns, $P > 0.05$, *$P \leq 0.05$, **$P \leq 0.01$, ***$P \leq 0.001$, ****$P \leq 0.0001$) assessed by two-way ANOVA (B, D, F, H) and unpaired *t*-test (I, J, K, L).

tumor cells pretreated with PL increased their sensitivity to NK cell-mediated cytotoxicity. Besides, there was an increased overall NK cell cytolysis at low ratios of NK: target cells in comparison with higher E: T ratios for Hela (Fig. 3D) and HepG2 (Fig. 3F) in contrast with A375 (Fig. 3B) and Huh7 (Fig. 3H).

To further establish the synergistic in vitro cytolytic effect of PL and NK cells on the tested tumor cells, we assessed the co-treatment of PL (at a dose where NK cell's viability is preserved) and NK cell on the tumor cells. Data showed a significant synergistic cytolytic increase between PL and NK cells compared to PL or NK cell treatment alone (Fig. 3I - L).

The observed variation in tumor cell sensitivity to NK cells cytotoxicity could result from the differences in NK cell-activating and inhibitory receptors' surface expression levels and ligands. These data demonstrate the immunomodulatory potential of PL, in addition to its antitumor effects.

3.4. Piperlongumine (PL) treatment induces ROS generation in tumors cells

Several studies have reported that PL can induce intracellular reactive oxygen species (ROS) accumulation as part of its antitumor activity [13,26,27]. We evaluated the level of intracellular ROS generation in tumor cells treated with increasing doses of PL. We observed an increase in ROS generation in a dose-dependent manner for all the tumor cells (Fig. 4A–D). As shown in Fig.4A, 1 μM of PL was sufficient to induce a significant increase in intracellular ROS in A375 cells compared to vehicle-treated cells. In contrast, only 4 and 8 μM of PL were required to generate significant intracellular ROS in Hela, HepG2, and Huh7 cells compared with their respective controls (Fig. 4B–4D). These data revealed that PL could induce elevated intracellular ROS generation due to its toxicity towards tumor cells.

Our data and those from other reports [10,12,28,29] showed that PL induces ROS in tumor cells by glutathione depletion as part of its anticancer effect; we explored the possibility of mitigating this effect in the presence of NAC (N-acetyl-L-cysteine)– a potent antioxidant which is known to inhibit ROS-dependent apoptosis [30,31]. Treatment of the tumor cells with increasing doses of PL in the presence of 2 mM NAC completely abrogated the elevated intracellular ROS initially observed (Fig. 4 A-D and Fig. 5 A-D). Since NAC is a precursor of intracellular cysteine and glutathione, its antioxidant activity ensues from its thiol's group direct redox potential or increasing glutathione levels in the cells [32]. Therefore, NAC can mitigate the ROS-inducing properties of PL.

3.4.1. Piperlongumine (PL) treatment induces accumulation of misfolded proteins and activates autophagy

Tumor cells have a heightened capacity for protein turnover to facilitate the correct protein folding, supporting their growth and metastasis. The ubiquitin–proteasome system (UPS) and the autophagy pathway constitute the protein degradative system –through their ability to clear and recycle misfolded proteins [33–35]. We reasoned whether the increased susceptibility to NK cell cytolysis after PL pretreatment was related to the alterations in the UPS system. We tested the effect of PL treatment on tumor cells to induce proteotoxic stress and disrupt the protein degradative pathways. As shown in Fig. 4E–H, PL treatment altered and impeded the UPS by accumulating misfolded proteins. In Fig. 4E–G, 2–8 μM of PL significantly induced misfolded protein accumulation in A375, Hela, and HepG2 cells compared to their controls as indicated by the SS portion of the immunoblot. However, 4–8 μM of PL was required to significantly induce misfolded protein in Huh7 cells (Fig. 4H).

To show the involvement of autophagy in PL-induced cytotoxicity, we examined a reliable autophagy marker – which is the conversion of LC3-I to LC3-II [36,37]. This conversion begins 12 h post-exposure to 2 μM of PL for A375 and HUH7 cells (Fig. 4I and L, respectively). In contrast, as early as eight (8) hours post-PL exposure was required for LC3 conversion for Hela and HepG2 cells (Fig. 4J and K, respectively). The LC3 conversion also increased with time for all the tumor cells (Fig. 4I–L). Taken together, our data suggest that PL possesses immunomodulatory potential via the impairment of the UPS by inducing the accumulation of misfolded proteins and activating the autophagic flux in PL-treated tumor cells.

3.5. Piperlongumine (PL) pretreatment of tumor cells enhances their NK cells' cytotoxicity via inducing ROS in tumor cells

Since tumor cells pretreated with PL increased their sensitivity to NK cell-mediated cytotoxicity by inducing ROS and impairing the Ubiquitin-Proteasome System and autophagy, we reasoned whether this enhanced NK cell killing of PL treated tumor cells can be abolished in the absence of these proteotoxic effects. NAC is a potent antioxidant and has also been shown to relieve ubiquitin–proteasome inhibition [38]. Therefore, we used NAC as both an antioxidant and proteasome agonist. Also, we used Bromhexine hydrochloride (BRH) as an autophagy agonist. The pretreatment of the tumor cells with PL in the presence or absence of these agonists (NAC and BRH) before NK cell cytolysis significantly abrogated PL's immunomodulatory effect in all the tumor cell lines (Fig. 5E–L, Supplementary Fig. 1A-H). Taken together, these data show that intrinsically, tumor cells display enhanced capacity to overcome increase ROS generation and maintain proteostasis to promote tumorigenesis, which PL can impede, leading to enhanced sensitivity of these tumor cells to NK cell killing.

3.6. Piperlongumine (PL) treatment increases the conjugation of NK cells and tumor cells

NK cell cytolysis against target cells is a multiple-step approach starting with the conjugation formation with its target cells [39]. We evaluated tumor cell engagement with NK cells upon PL treatment. Our data showed a significant increase in conjugation between NK and PL treated tumor cells than their controls (Fig. 6A–H). Seven (7) minutes of co-incubation in PL-treated A375 and Huh7 cells resulted in a significant increase in NK-tumor conjugate formation (Fig. 6B and H). However, PL-treated Hela cells showed significant conjugate formation with NK cells after 15 min of co-incubation (Fig. 6D). PL-treated HepG2 cells required 30 min of co-incubation with NK cells to show significant conjugate formation (Fig. 6F). This observation indicates that Piperlongumine enhances the appearance of conjugation between NK cells and tumor cells.

3.6.1. Piperlongumine (PL) pretreatment enhances NK cell triggering receptors' expression on NK (YTS) and tumor cells

Given that our in vitro findings showed the antitumor activities of PL alone by its ability to induce pro-apoptotic proteins, induce ROS, autophagy, and misfolded protein accumulation. We wanted to find more mechanistic insight into the enhanced NK cell killing of the PL-treated tumor cell lines. NK cell activity is dependent on a balance between its activating and inhibitory surface receptors [40], the preincubation of NK (YTS) cells with PL or DMSO control for 20 hours, followed by flow cytometry assessment of the level of activating surface receptors showed that PL was able to slightly enhance the expression of CD28 (the primary activating receptor that stimulates cytotoxicity of NK (YTS) cells) in comparison to vehicle-only treated controls (Fig. 7A). Interestingly, there was a relatively low surface expression of other activating receptors (CD226, FASL, LFA-1, NKG2D, NKP46) on the NK (YTS) cells with no observable differences between PL and vehicle-treated groups (Fig. 7A). All the four target cells were also tested for their expression pattern of CD80, CD86 (ligands for CD28), and CD112 (another NK cell-activating ligand). All the tumor cell lines showed varying expression patterns, with PL-treated groups displaying a slightly higher surface expression compared to the control (Fig. 7B-E). The enhanced expression of CD28 (on NK cell) and its ligands (CD80 and CD86 –on these tumor cells) suggests that CD28 signaling may also be involved in the

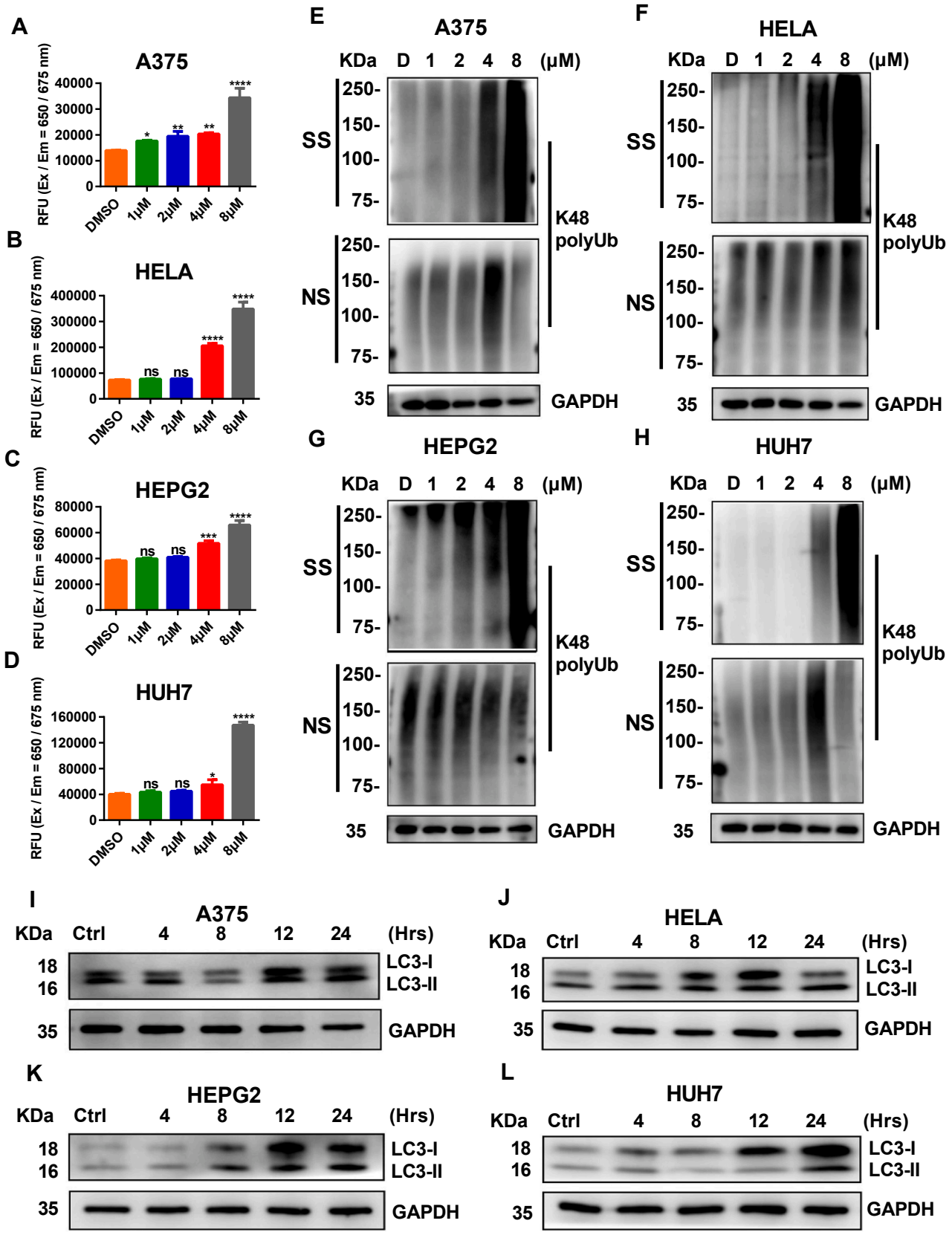

Fig. 4. Treatment of tumors with Piperlongumine (PL) generates ROS, induces misfolded proteins, and impedes autophagy. Assessment of total reactive oxygen species (ROS) generation in Piperlongumine (PL) treated tumor cells. Increasing doses (1–8 μM) of PL and DMSO control were exposed to tumor cells for 24 hours (A) A375 (B) HELA (C) HEPG2 (D) HUH7. (E–H) the level of K48 poly Ub conjugates in increasing dose (1–8 μM) of PL treated and control cells (E) A375 (F) HELA (G) HEPG2 (H) HUH7. (I–L) the formation of autophagic protein marker LC3-II increases with time in response to 2 μM of PL treatment of tumor cells. (I) A375 (J) HELA (K) HEPG2 (L) HUH7. Relative Fluorescence Units (RFU) are expressed as mean ± SD for each group (A, B, C, D). ($n \geq 3$ replicates) from three independent experiments. (not significant ns, $P > 0.05$, *$P \leq 0.05$, **$P \leq 0.01$, ***$P \leq 0.001$, ****$P \leq 0.0001$) assessed by unpaired *t*-test. (E-L) representative immunoblots.

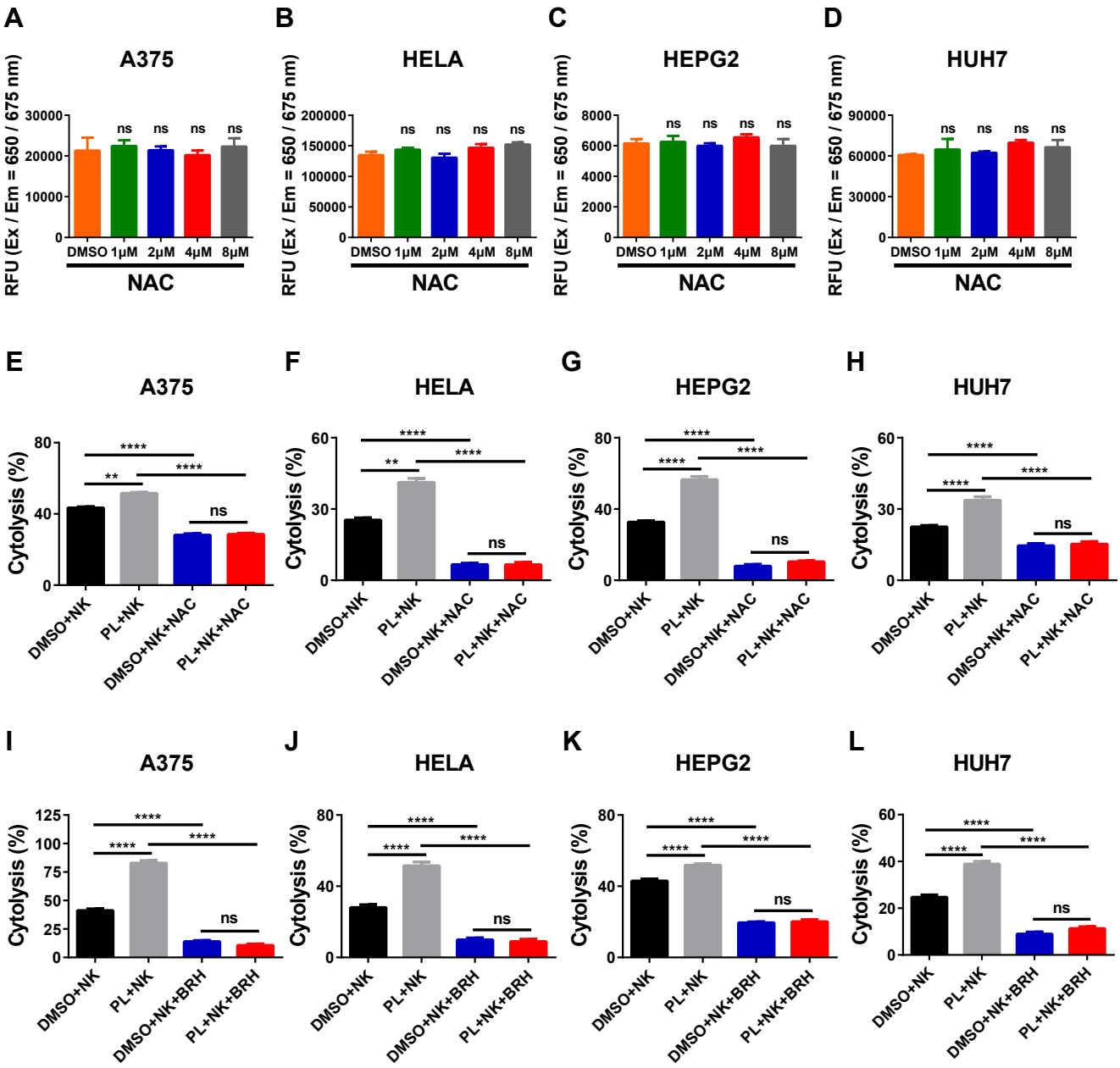

Fig. 5. Abrogation of the enhanced NK cell cytolysis of Piperlongumine (PL) Pretreated Tumor cells with antioxidant, autophagy, and proteasome agonists. (A-D) Assessment of total ROS upon treatment of tumor cells with increasing doses (1–8 μM) of PL and DMSO control for 24 hours in the presence of 2 mM N-Acetyl Cysteine (NAC). (A) A375 (B) HELA (C) HEPG2 (D) HUH7. Representative fluorescence spectra, Relative Fluorescence Units (RFU) are expressed as mean ± SD for each group (A, B, C, D). In vitro evaluation of NK cell cytotoxicity of PL or DMSO treated tumor cells with or without (E-H) N-Acetyl Cysteine (antioxidant, proteasome agonist), (I-L) Bromhexine hydrochloride (BRH) autophagy agonist. The cells were pretreated with 2 μM of PL or DMSO control in the presence or absence of NAC (2 mM) and BRH (2 mM) for 20 hours prior to NK cell cytolysis using the REAL-TIME Cell Analyzer (RTCA). (E, I) A375, (F, J) HELA, (G, K) HEPG2, (H, L) HUH7. Percentage cytolysis is expressed as mean ± SD for E: T ratio (9:1). ($n \geq 4$ replicates) from three independent experiments (A-L). (not significant ns, $P > 0.05$, *$P \leq 0.05$, **$P \leq 0.01$, ***$P \leq 0.001$, ****$P \leq 0.0001$) assessed by unpaired *t*-test.

cytolytic activity of NK (YTS) cells on the tumor cells.

3.7. Piperlongumine (PL) treatment showed better control of tumor in vivo

Based on the above in vitro findings, we hypothesized that PL could facilitate immunity against NK –sensitive MHC-I –deficient tumor as well as MHC-I –sufficient tumor growth in vivo. First, we investigated whether PL pretreatment (at the same dosage used for the *in vitro* cytolytic assay) could also suppress tumor growth *in vivo*. As expected, PL pretreatment suppressed RMA-S tumor growth relative to vehicle-treated control (Fig. 8A-D), suggesting that the effects of PL on tumor cells alone could render the tumor-suppressing effects we observed.

We then sought to investigate the therapeutic benefits of PL administration in suppressing tumor growth using different tumor models: RMA-S (MHC-I –deficient tumor cell), B16F10, and CT26 (MHC-I –sufficient) tumor models. As expected, the therapeutic administration of Piperlongumine to tumor-bearing mice had reduced tumor growth compared to controls (Fig. 8E-P). Additionally, body weights were unaltered, indicating a low or no systemic toxicity of the PL therapy (Fig. 8G, K, O). Collectively, these data suggest that Piperlongumine could therapeutically suppress both NK –sensitive MHC-I –deficient and

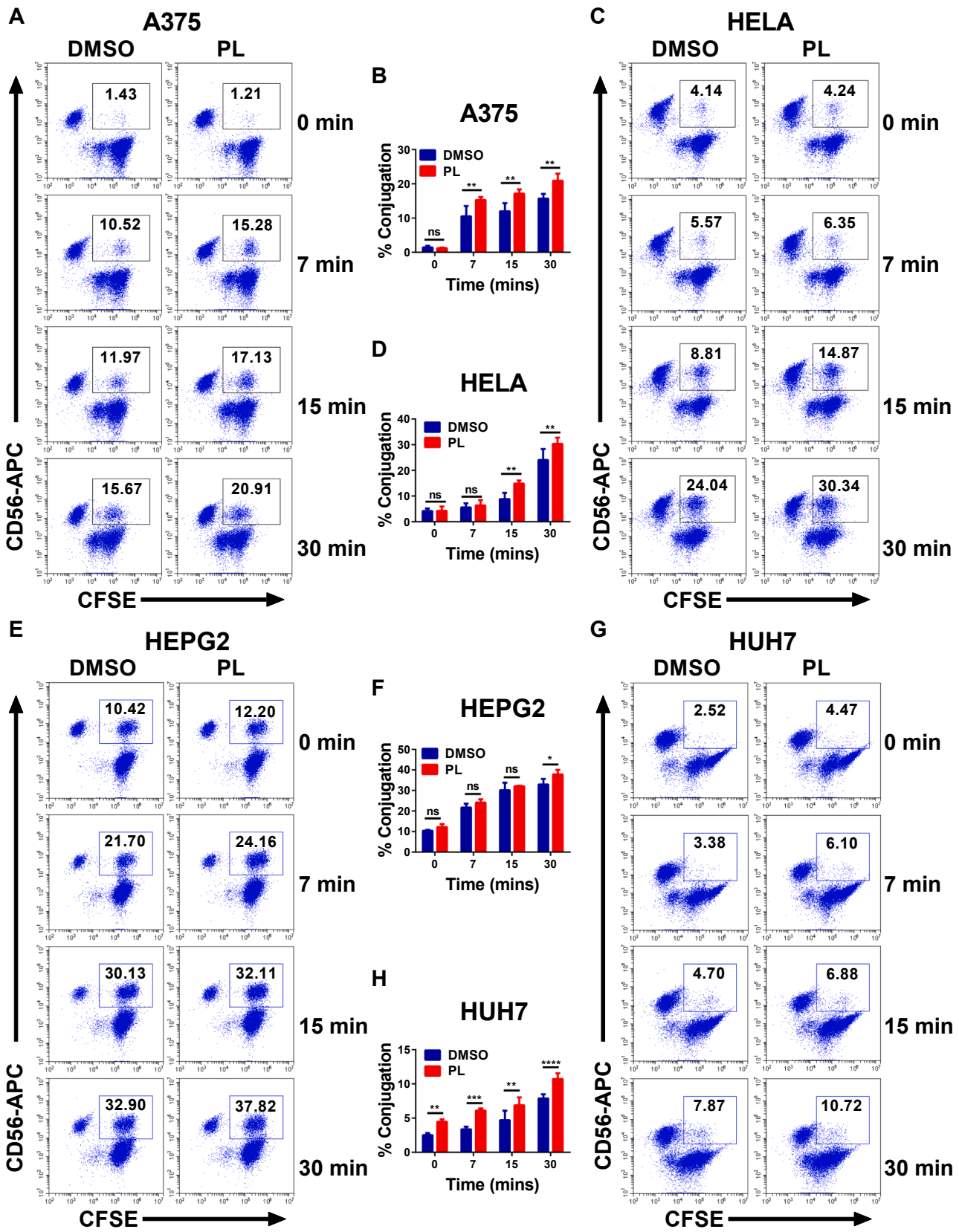

Fig. 6. Piperlongumine (PL) Pretreatment of Tumors increases their conjugation with NK effector cell. Piperlongumine (PL) pretreated tumor cells for 24 hours, labeled with CFSE, and co-incubated with CD56-APC labeled NK(YTS) cells for the indicated times. Conjugates formation between NK (YTS) and target cells (A, C, E, G) are indicated as the double-positive population as assessed by flow cytometry. (A, B) A375, (C, D) HELA, (E, F) HEPG2, (G, H) HUH7. Representative dot plots (A, C, E, G), Statistical analysis of the conjugates formed at different time points (B, D, F, H). Percentage conjugation is expressed as mean ± SD ($n \geq 4$ replicates) from three independent experiments. Statistical significance was assessed by a two-way ANOVA (B, D, F, H).

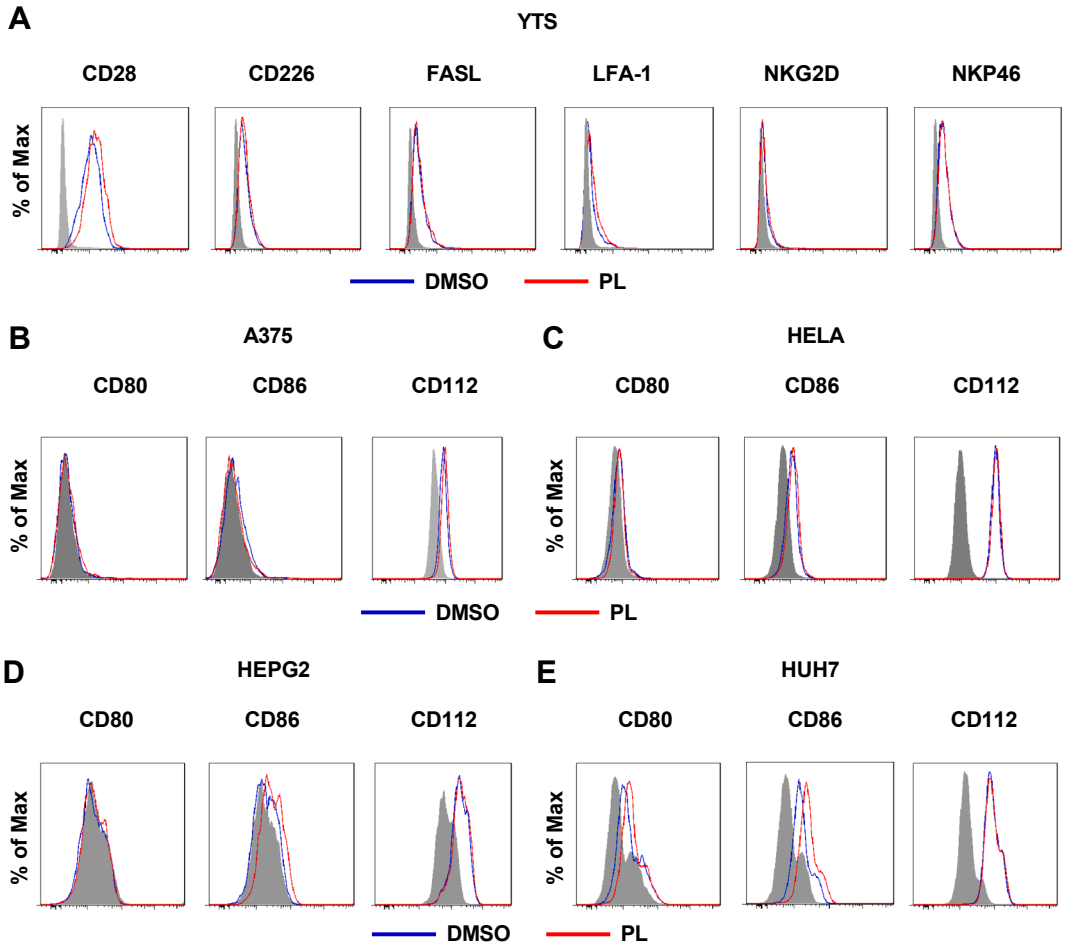

Fig. 7. Effect of Piperlongumine (PL) Pretreatment on enhancing NK cell-activating receptors. YTS and Tumor cells were pretreated with 2 μM of Piperlongumine (Red solid lines) or DMSO control (Blue solid lines) for 20 hours prior to assessment for the specified activating receptors with the corresponding IgG Isotype controls (grey shaded regions) and analyzed by flow cytometry. (A) Assessment of selected surface activating receptors expression on YTS cell; (B-E) surface expression of NK cells activating ligands on tumor cells. (B) A375, (C) HELA, (D) HEPG2, (E) HUH7. Data is representative of three independent experiments.

MHC-I –sufficient tumor growth in vivo.

3.7.1. Piperlongumine (PL) suppressed tumor growth in an NK cell-dependent manner

Based on our in vivo findings on PL suppression of NK –sensitive MHC-I –deficient (RMA-S) tumor model, we proceeded to confirm further the involvement of NK cells in the in vivo antitumor activity of PL. To this end, PL significantly lost the therapeutic benefits in NK-depleted C57BL/6J mice subcutaneously injected with RMA-S and B16F10 cells (Fig. 8Q-T, Supplementary Fig. 1I-L), which indicates that PL in vivo antitumor therapeutic activity is NK cell-dependent.

3.7.2. Piperlongumine (PL) therapy enhances NK cell activation in vivo

To further investigate the immune cells' in vivo PL engagement to suppress tumor growth, we assessed the population of splenic NK cells from the B16F10 tumor-bearing mice treated with PL with their untreated control. As shown in Fig. 9A, a significantly higher percentage of NK cells in the treatment group than the control was observed. CD69 and CD107a two surface markers that depict NK cell activation and degranulation were higher in the treated group than the control (Fig. 9 B, C). The role of NKG2D in the control of tumors and infection has been well documented [40,41]. Similarly, assessment of the activating receptor NKG2D also showed that PL promoted the expression of NKG2D + NK cells. Therefore, the data suggest that PL therapy favors NK cell activation to suppress tumor growth in vivo.

4. Discussion

Piperlongumine (PL) has been reported as a promising antitumor compound both in vitro and in vivo [42–45]; and characterized selective tumor killing with minimal effect on normal cells [9,15]. This study focused on evaluating the antitumor and immunomodulatory roles of PL on selected tumor cell lines. We observed that PL induces apoptosis in all tested tumor cells, with an associated decrease in the tumor cell viability after 24 hours treatment in a dose-dependent manner (Fig. 1B–I). Our findings are in line with works of literature [42–44,46]. Also, we observed that PL could induce apoptosis via the expression of caspase-3 activity; this observation is also in line with earlier reports of possible mechanisms of apoptosis of PL on tumor cells [14,47].

On the other hand, PL concentration less than 8 μM showed no detrimental effect on NK (YTS) cell viability; however, 8 μM slightly induced apoptosis with decreased cell viability compared to the vehicle-only treated control. Similarly, PL showed minimal effect on the viability of four normal cell lines (Fig. 1L-O). Our findings corroborate with the report on the selective tumor killing of PL and not on normal cells [9,15].

Consistent with our apoptosis assay data, PL also demonstrated potent anti-proliferative activity on all treated tumors with significant inhibition at all tested dosages (Fig. 2A–H); as little as 1 μM was capable of eliciting significant inhibition of cell proliferation in all the tumor cells. Our finding is in line with earlier reports showing the growth inhibitory effect of PL on tumor cells via cell cycle arrest [11,48,49].

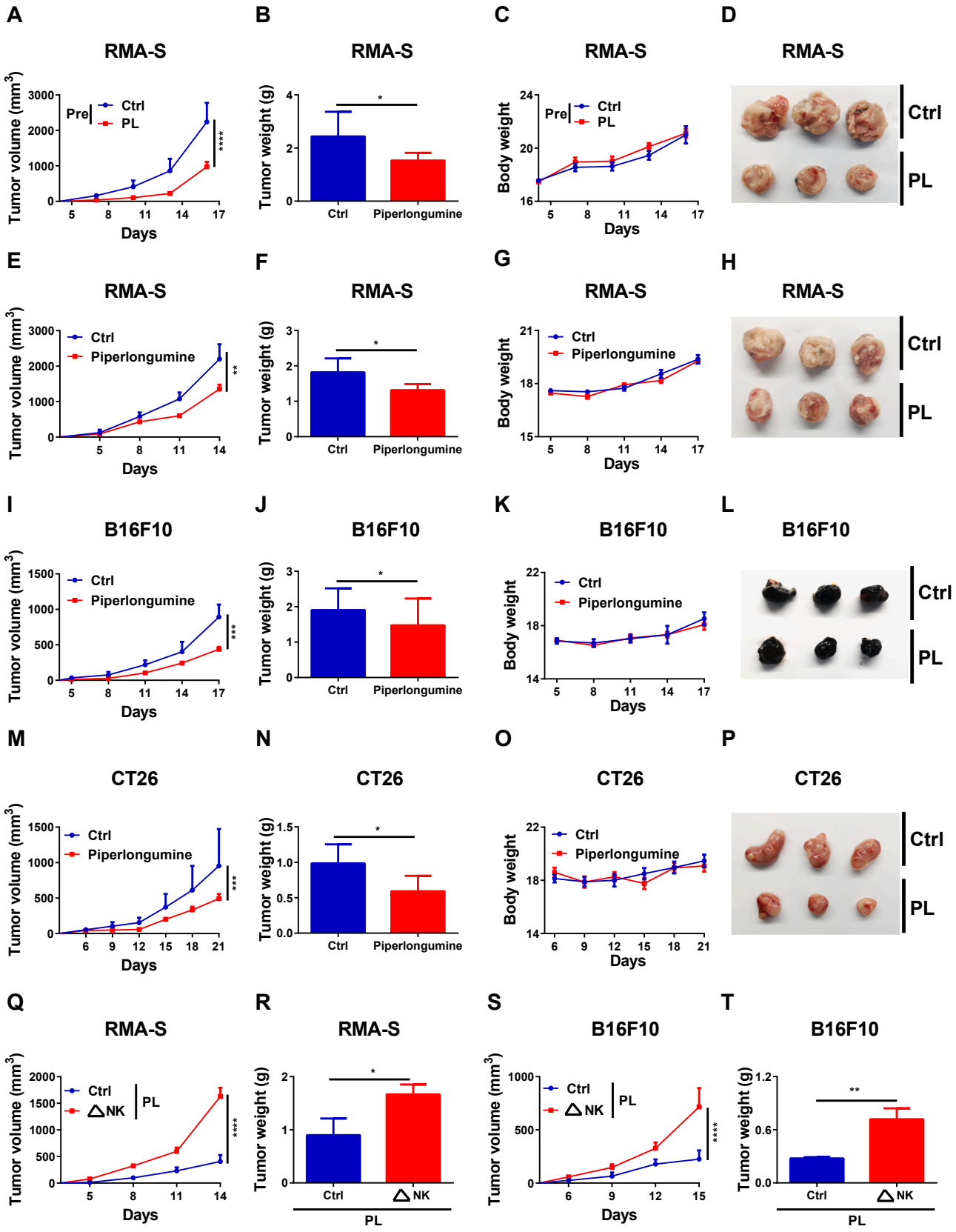

Fig. 8. Piperlongumine (PL) treatment enhances better control of Tumor growth. Pretreated tumor cells prior to mice inoculation (A-D). Assessment of tumor growth kinetic (Tumor growth curve, Tumor weight, Bodyweight and, Tumor images at the end of the experiment), upon PL pretreatment of tumor cells and PL therapy (A-D; E-H, RMA-S tumor model: 1x 10^6 cells), (I-L, B16F10 tumor model: 2x 10^5 cells), (M–P, CT26 tumor model: 2x 10^5 cells). (Q-T) NK cell depletion (ΔNK) one day prior to tumor inoculation. Assessment of Tumor growth curve, Tumor weight for (Q, R) RMA-S, and (S, T) B16F10 tumor models.

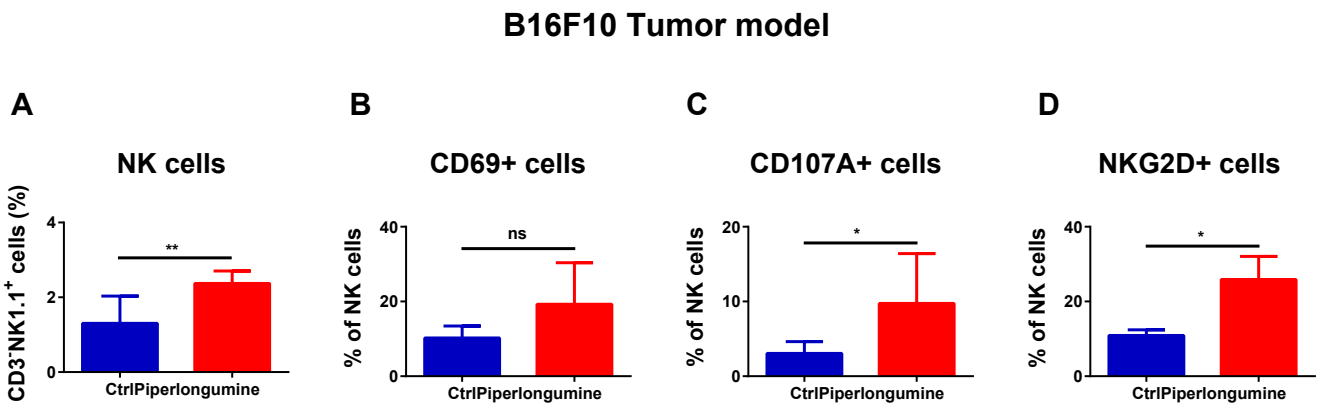

Fig. 9. Piperlongumine (PL) therapy promotes splenic NK cell activation. Assessment of splenic NK cell activation and degranulation status in a B16F10 tumor model. (A) percentage of splenic NK cells; (B) percentage of $CD69^+$ NK cells; (C) percentage of $CD107A^+$ NK cells; (D) percentage of $NKG2D^+$ NK cells. Data are expressed as mean ± SD ($n \geq 6$ replicates) from two independent experiments. Statistical significance was assessed by an unpaired *t*-test. (not significant ns, $P > 0.05$, $^*P \leq 0.05$, $^{**}P \leq 0.01$).

Several other reports have demonstrated that PL can induce cell cycle arrest, leading to the inhibition of tumor cells' angiogenesis and metastasis [14,27].

We further evaluated the potential of PL to serve as an immunomodulatory agent. Our findings showed that PL pretreated tumor cells before NK cell cytolysis increase their killing (Fig. 3A–H). A low dose of PL (2 μM) pretreatment of tumor cells was sufficient to significantly enhance their cytolysis by NK cells at the tested E:T ratios. Additionally, the co-treatment of these tumor cells with PL and NK cells displayed a significant synergistic cytolytic activity compared to PL or NK cell treatment alone (Fig. 3I–L). Since NK cells are particularly effective in eliminating tumor cells via many mechanisms [3], it is possible that PL acted as an immunomodulatory agent.

Immunomodulators have the potential to activate cytotoxic effector cells, including NK cells and cytotoxic T lymphocytes. PL is also capable of inducing stress in tumor cells [16,28]: and stress induction can elicit the release of stress molecules such as damage-associated molecular patterns (DAMPs), which can trigger immune effector cell function [7]. Besides, they can also modulate the surface expression pattern of NK cell-activating and inhibitory ligands on tumor cells, thereby rendering them immunogenic to NK cell cytotoxicity [8].

There is a heightened generation of oxidative stress in tumor cells compared to normal cells, with tumor cells having to continuously fine-tune the level of their intracellular ROS signaling [50,51]. Paradoxically, elevated ROS accumulation has been implicated in inducing growth arrest and apoptosis [52]. Increase ROS levels in cancer cells make them sensitive to ROS-inducing agents [53,54]; thus, stimulating ROS generation in tumors could be a potential therapeutic strategy. This study observed that PL treatment increased ROS levels for all the tumor cells (Fig. 4A–D). Our observation agrees with other studies on PL's ability to induce elevated ROS levels in tumor cells [13,16,55,56]. The ROS-inducing anticancer effect of PL has been attributed to its ability to modulate the activity of glutathione S-transferase (GSTP1) as well as depletion of glutathione (GSH) levels [10,12]. The increased intracellular ROS generation of PL was abolished in the presence of NAC –a precursor of intracellular cysteine and glutathione (Fig. 5A-D). This finding agrees with the report that NAC can restore glutathione levels in the cell [32].

Tumor cells usually possess increased protein quality control to accommodate their continuous growth and metastasis. The unique role of the protein degradative system in tumors has been well characterized [22,35], and the disruption of the protein quality control process is harmful to cellular growth. We demonstrated that PL treatment induced the accumulation of misfolded proteins and hindered the ability of the ubiquitin–proteasome system (UPS) to degrade them (Fig. 4E–H). Both the UPS and autophagy pathways are associated with their ability to recycle misfolded proteins [33–35] and play protein quality control roles. Our findings showed that PL-treated tumor cells had increased autophagic flux (Fig. 4I–L). Moderate autophagy is involved in homeostasis to environmental stress [57]; however, high or inappropriate autophagic flux can lead to cell death [58].

There is a correlation between efficient clearance of misfolded proteins and strong antioxidants defense during tumorigenesis. The accumulation of misfolded proteins is usually accompanied by high oxidative stress and growth inhibition [22]. Since elevated ROS can damage proteins, including other cellular components, increased oxidative stress and accumulation of misfolded proteins can result in a vicious cycle that may explain our observations for PL's role in the current study.

Report has shown that the suppression of the protein quality control system sensitizes tumors to NK cell cytolysis [60]. Also, the inhibition of the ubiquitin–proteasome system has been shown to increase the surface expression of immunogen, enhancing tumor cells' susceptibility to NK cell cytotoxicity [61]. In the current study, we observed that PL could induce disruption of the UPS as evident by the misfolded protein accumulation; this phenomenon may explain the increased NK cells cytotoxicity of PL pretreated tumor cells.

Our data showed that the enhanced NK cell cytolysis of PL treated tumor cells can be abrogated in the presence of agents that facilitate the removal of intracellular ROS and alleviate the proteotoxic stress-induced by PL (antioxidant, autophagy and proteasome agonists) (Fig. 5E–L). NAC was able to abrogate the ROS-inducing and proteasome-inhibiting effects of PL. Our findings agree with the report that showed NAC could directly bind to PL, thereby interfering in its ROS generation and proteasome inhibition [38]. Also, the use of bromhexine hydrochloride (an autophagy agonist) to abrogate PL proteotoxic stress on pretreated tumor cells aligns with an earlier report on the ability of bromhexine hydrochloride to clear protein aggregates (such as tau aggregates) in tumor cells [59]. Therefore, the removal of these proteotoxic stress induced by PL abolished the enhanced NK cell cytotoxicity.

To further substantiate PL's antitumor role, we assess tumor cell engagement upon PL treatment; our data showed a significant increase in conjugation between NK and PL treated tumor cells (Fig. 6AI–H). NK cytolysis of tumor cells is a multi-step approach, including conjugation formation with its target cells via adhesion molecules [39]. This may also explain in part the increased NK cell cytolysis of PL-pretreated tumor cells. Our observation is consistent with an earlier report, which shows that conjugate formation between lymphocyte-activated killer cells and bladder cancer cell lines is a prerequisite for tumor cell cytotoxicity [60]. Several other reports have demonstrated the importance of conjugation between tumor and the effector cells for tumor cytotoxicity [60–64].

Given the association of NK cell cytotoxicity relative to the balance of

activating and inhibitory signals from its surface receptors, evaluation of the activating surface receptors by FACS revealed a slight increase in the expression of CD28 receptor in PL treated NK (YTS) cells compared to the control (Fig. 7A); however, there was a relatively low surface expression of other activating receptors. Also, the expression of ligands for CD28 (CD80, CD86) on the tumor cells, albeit with a slightly higher expression on PL treated tumor cells, may explain the increased cytolysis in the treatment group, which further affirms the immunomodulatory role of PL. Furthermore, this observation also suggests that CD28 signaling may be involved in the cytolytic activity of NK (YTS) cells on the tumor cells. Our findings are consistent with reports that show that CD28 signaling is the major cytolytic signal for NK (YTS) cells in tumor cells that express their ligands. [65,66]. This suggests that PL also modulates NK cells' antitumor killing by enhancing the expression of their activating receptor.

Interestingly, the tumor cell lines showed varying expression patterns of NK cell-activating ligands; PL treatment also slightly favored the increased surface expression of these ligands compared to the control (Fig. 7B-E); suggesting that PL can modulate the surface expression pattern of NK cell-activating receptors and their corresponding activating ligands on tumor cells, thereby rendering them immunogenic to NK cell cytotoxicity.

Our in vivo study highlights Piperlongumine's potent ability to induce both cytostatic and cytotoxic anticancer effects (Fig. 8A-D). The pretreatment of tumor cells prior to inoculation further emphasized PL's cytostatic potential as it significantly suppressed tumor growth relative to vehicle-treated control. Besides, the ability of PL to harness host immune effector mechanisms and control tumor growth was revealed in the C57BL/6 mice bearing prototypical NK cell-sensitive target cells (RMA-S) and other MHC-I –sufficient tumor models in vivo (Fig. 8E-P).

Furthermore, the loss of the therapeutic benefit of PL observed following NK cell depletion (Fig. 8Q-T) indicates NK cells' involvement in PL antitumor activity, suggesting that PL in vivo antitumor therapeutic activity is NK cell-dependent. Since there was no loss in body weights for the mice, this suggests that PL therapy can be well tolerated with little or no systemic toxicity.

Our in vivo finding is consistent with the work of Sunila and Kuttan, who demonstrated the in vivo immunomodulatory role of PL administration. In their study, PL significantly reduced tumor development with a concomitant increase in cytotoxic lymphocytes population in a Dalton's Lymphoma mouse model. The authors opined that PL's immunomodulatory activity might result from its ability to stimulate humoral and cell-mediated immune responses [67]. Finally, the promotion of splenic NK cell activation as observed in our study (Fig. 9A-D) further establishes that PL may improve NK cell antitumor functions in PL-treated tumor-bearing mice possibly by promoting tumor-associated NK cell recruitment.

Although the current study is not exhaustive, it presents an avenue for further investigations into NK cells' involvement and other immune cells in PL antitumor activity with other potential underlying mechanisms.

The identification and use of novel antineoplastic compounds (such as PL) as immunomodulatory agents to augment conventional chemotherapy care can be explored to overcome the challenges associated with traditional chemotherapies and drug resistance. These immunomodulators' ability to engage endogenous antitumor immunity upon changing tumor cells' immunogenicity holds many promises. To achieve complete tumor remission, the use of natural products as immunomodulators capable of eliciting antitumor activities via multiple mechanisms of action while enhancing cytotoxic lymphocytes' effector functions (CTLs), including NK cells, is required.

Funding

This work was funded by the National Key R&D Program of China (2019YFA0906100 and 2020YFA0710802), the Natural Science Foundation of China (82071768), the Natural Science Foundation of Guangdong Province (2019A1515011412), Shenzhen Basic Science Research Project (JCYJ20170818164619194), Shenzhen Basic Science Research Project (JCYJ20170413153158716), Special funds for major science and technology of Guangdong province (2019B020201014), and Nanshan pilot team project (LHTD20A360004).

Acknowledgments

Sponsored by UCAS Scholarship for International Students.

Author contributions

L.O.A and J.B designed the experiments, analyzed the data, and wrote the manuscript; L.O.A performed the experiments; L.C validated the investigation and reviewed the first draft; X.W supervised the project and oversaw the writing process.

Appendix A. Supplementary material

Supplementary data to this article can be found online at https://doi.org/10.1016/j.intimp.2021.107658.

References

[1] E. Vivier, E. Tomasello, M. Baratin, T. Walzer, S. Ugolini, Functions of natural killer cells, Nat. Immunol. 9 (5) (2008) 503–510.
[2] E. Vivier, D.H. Raulet, A. Moretta, M.A. Caligiuri, L. Zitvogel, L.L. Lanier, W. M. Yokoyama, S. Ugolini, Innate or adaptive immunity? The example of natural killer cells, 331, Science, New York, N.Y., 2011, pp. 44–49.
[3] L.O. Afolabi, A.O. Adeshakin, M.M. Sani, J. Bi, X. Wan, Genetic reprogramming for NK cell cancer immunotherapy with CRISPR/Cas9, Immunology 158 (2) (2019) 63–69.
[4] G. Habif, A. Crinier, P. Andre, E. Vivier, E. Narni-Mancinelli, Targeting natural killer cells in solid tumors, Cell. Mol. Immunol. 16 (5) (2019) 415–422.
[5] J. Bi, Z. Tian, NK cell dysfunction and checkpoint immunotherapy, Front. Immunol. 10 (2019) 1999.
[6] Q. Huang, M. Huang, F. Meng, R. Sun, Activated pancreatic stellate cells inhibit NK cell function in the human pancreatic cancer microenvironment, Cell. Mol. Immunol. 16 (1) (2019) 87–89.
[7] L. Bracci, G. Schiavoni, A. Sistigu, F. Belardelli, Immune-based mechanisms of cytotoxic chemotherapy: implications for the design of novel and rationale-based combined treatments against cancer, Cell Death Differ. 21 (1) (2014) 15–25.
[8] A. Zingoni, C. Fionda, C. Borrelli, M. Cippitelli, A. Santoni, A. Soriani, Natural killer cell response to chemotherapy-stressed cancer cells: role in tumor immunosurveillance, Front. Immunol. 8 (2017) 1194.
[9] X.-X. Xiong, J.-M. Liu, X.-Y. Qiu, F. Pan, S.-B. Yu, X.-Q. Chen, Piperlongumine induces apoptotic and autophagic death of the primary myeloid leukemia cells from patients via activation of ROS-p38/JNK pathways, Acta Pharmacol. Sin. 36 (3) (2015) 362–374.
[10] W. Harshbarger, S. Gondi, S.B. Ficarro, J. Hunter, D. Udayakumar, D. Gurbani, W. D. Singer, Y. Liu, L. Li, J.A. Marto, K.D. Westover, Structural and biochemical analyses reveal the mechanism of glutathione S-transferase Pi 1 inhibition by the anti-cancer compound piperlongumine, J. Biol. Chem. 292 (1) (2017) 112–120.
[11] L. Zhou, M. Li, X. Yu, F. Gao, W. Li, Repression of hexokinases II-mediated glycolysis contributes to piperlongumine-induced tumor suppression in non-small cell lung cancer cells, Int. J. Biol. Sci. 15 (4) (2019) 826–837.
[12] H. Dhillon, S. Chikara, K.M. Reindl, Piperlongumine induces pancreatic cancer cell death by enhancing reactive oxygen species and DNA damage, Toxicol. Rep. 1 (2014) 309–318.
[13] K. Karki, E. Hedrick, R. Kasiappan, U.-H. Jin, S. Safe, Piperlongumine Induces Reactive Oxygen Species (ROS)-Dependent Downregulation of Specificity Protein Transcription Factors, Cancer Prev. Res. (Phila.) 10 (8) (2017) 467–477.
[14] S. Thongsom, W. Suginta, K.J. Lee, H. Choe, C. Talabnin, Piperlongumine induces G2/M phase arrest and apoptosis in cholangiocarcinoma cells through the ROS-JNK-ERK signaling pathway, Apoptosis : Int. J. program. cell Death 22 (11) (2017) 1473–1484.
[15] U. Bharadwaj, T.K. Eckols, M. Kolosov, M.M. Kasembeli, A. Adam, D. Torres, X. Zhang, L.E. Dobrolecki, W. Wei, M.T. Lewis, B. Dave, J.C. Chang, M.D. Landis, C. J. Creighton, M.A. Mancini, D.J. Tweardy, Drug-repositioning screening identified piperlongumine as a direct STAT3 inhibitor with potent activity against breast cancer, Oncogene 34 (11) (2015) 1341–1353.
[16] Q. Zhang, W. Chen, X. Lv, Q. Weng, M. Chen, R. Cui, G. Liang, J. Ji, Piperlongumine, a novel TrxR1 inhibitor, induces apoptosis in hepatocellular carcinoma cells by ROS-mediated ER stress, Front. Pharmacol. 10 (2019) 1180.
[17] A.J. Christiansen, A. West, K.-M. Banks, N.M. Haynes, M.W. Teng, M.J. Smyth, R. W. Johnstone, Eradication of solid tumors using histone deacetylase inhibitors combined with immune-stimulating antibodies, PNAS 108 (10) (2011) 4141–4146.

[18] M.R. Shurin, H. Naiditch, D.W. Gutkin, V. Umansky, G.V. Shurin, ChemoImmunoModulation: immune regulation by the antineoplastic chemotherapeutic agents, Curr. Med. Chem. 19 (12) (2012) 1792–1803.
[19] R.B. Delconte, T.B. Kolesnik, L.F. Dagley, J. Rautela, W. Shi, E.M. Putz, K. Stannard, J.-G. Zhang, C. Teh, M. Firth, T. Ushiki, C.E. Andoniou, M.A. Degli-Esposti, P.P. Sharp, C.E. Sanvitale, G. Infusini, N.P.D. Liau, E.M. Linossi, C.J. Burns, S. Carotta, D.H.D. Gray, C. Seillet, D.S. Hutchinson, G.T. Belz, A.I. Webb, W. S. Alexander, S.S. Li, A.N. Bullock, J.J. Babon, M.J. Smyth, S.E. Nicholson, N. D. Huntington, CIS is a potent checkpoint in NK cell-mediated tumor immunity, Nat. Immunol. 17 (7) (2016) 816–824.
[20] P. Di Fazio, R. Montalbano, D. Neureiter, B. Alinger, A. Schmidt, A.L. Merkel, K. Quint, M. Ocker, Downregulation of HMGA2 by the pan-deacetylase inhibitor panobinostat is dependent on hsa-let-7b expression in liver cancer cell lines, Exp. Cell Res. 318 (15) (2012) 1832–1843.
[21] S. Lebourgeois, A. Fraisse, C. Hennechart-Collette, L. Guillier, S. Perelle, S. Martin-Latil, Development of a real-time cell analysis (RTCA) method as a fast and accurate method for detecting infectious particles of the adapted strain of hepatitis a virus, Front. Cell. Infect. Microbiol. 8 (2018) 335.
[22] L. Chen, M.D. Brewer, L. Guo, R. Wang, P. Jiang, X. Yang, Enhanced degradation of misfolded proteins promotes tumorigenesis, Cell. Rep. 18 (13) (2017) 3143–3154.
[23] L. Guo, B.I. Giasson, A. Glavis-Bloom, M.D. Brewer, J. Shorter, A.D. Gitler, X. Yang, A cellular system that degrades misfolded proteins and protects against neurodegeneration, Mol. Cell 55 (1) (2014) 15–30.
[24] D.N. Burshtyn, C. Davidson, Natural killer cell conjugate assay using two-color flow cytometry, Methods in molecular biology (Clifton, N.J.) 612 (2010) 89–96.
[25] A.O. Adeshakin, W. Liu, F.O. Adeshakin, L.O. Afolabi, M. Zhang, G. Zhang, L. Wang, Z. Li, L. Lin, Q. Cao, D. Yan, X. Wan, Regulation of ROS in myeloid-derived suppressor cells through targeting fatty acid transport protein 2 enhanced anti-PD-L1 tumor immunotherapy, Cell. Immunol. 362 (2021), 104286.
[26] J. Li, C.C. Sharkey, M.R. King, Piperlongumine and immune cytokine TRAIL synergize to promote tumor death, Sci. Rep. 5 (2015) 9987.
[27] J.-L. Roh, E.H. Kim, J.Y. Park, J.W. Kim, M. Kwon, B.-H. Lee, Piperlongumine selectively kills cancer cells and increases cisplatin antitumor activity in head and neck cancer, Oncotarget 5 (19) (2014) 9227–9238.
[28] H. Dhillon, Mechanisms of piperlongumine-induced cancer cell death, North Dakota State University (2015).
[29] S. Pei, M. Minhajuddin, K.P. Callahan, M. Balys, J.M. Ashton, S.J. Neering, E. D. Lagadinou, C. Corbett, H. Ye, J.L. Liesveld, K.M. O'Dwyer, Z. Li, L. Shi, P. Greninger, J. Settleman, C. Benes, F.K. Hagen, J. Munger, P.A. Crooks, M. W. Becker, C.T. Jordan, Targeting aberrant glutathione metabolism to eradicate human acute myelogenous leukemia cells, J. Biol. Chem. 288 (47) (2013) 33542–33558.
[30] J.F. Curtin, M. Donovan, T.G. Cotter, Regulation and measurement of oxidative stress in Apoptosis, J. Immunol. Methods 265 (1–2) (2002) 49–72.
[31] A.J. McGowan, R.S. Fernandes, A. Samali, T.G. Cotter, Antioxidants and apoptosis, Biochem. Soc. Trans. 24 (1) (1996) 229–233.
[32] S.Y. Sun, N-acetylcysteine, reactive oxygen species and beyond, Cancer Biol. Ther. 9 (2) (2010) 109–110.
[33] Y.E. Kim, M.S. Hipp, A. Bracher, M. Hayer-Hartl, F.U. Hartl, Molecular chaperone functions in protein folding and proteostasis, Annu. Rev. Biochem. 82 (2013) 323–355.
[34] J. Tyedmers, A. Mogk, B. Bukau, Cellular strategies for controlling protein aggregation, Nat. Rev. Mol. Cell Biol. 11 (11) (2010) 777–788.
[35] L. Zhang, L.O. Afolabi, X. Wan, Y. Li, L. Chen, Emerging roles of tripartite motif-containing family proteins (TRIMs) in eliminating misfolded proteins, Front Cell. Dev. Biol. 8 (2020) 802.
[36] Y. Kabeya, N. Mizushima, T. Ueno, A. Yamamoto, T. Kirisako, T. Noda, E. Kominami, Y. Ohsumi, T. Yoshimori, LC3, a mammalian homologue of yeast Apg8p, is localized in autophagosome membranes after processing, EMBO J. 19 (21) (2000) 5720–5728.
[37] N. Mizushima, Autophagy: process and function, Genes Dev. 21 (22) (2007) 2861–2873.
[38] M. Halasi, M. Wang, T.S. Chavan, V. Gaponenko, N. Hay, A.L. Gartel, ROS inhibitor N-acetyl-L-cysteine antagonizes the activity of proteasome inhibitors, Biochem. J. 454 (2) (2013) 201–208.
[39] E.M. Mace, P. Dongre, H.T. Hsu, P. Sinha, A.M. James, S.S. Mann, L.R. Forbes, L. B. Watkin, J.S. Orange, Cell biological steps and checkpoints in accessing NK cell cytotoxicity, Immunol. Cell Biol. 92 (3) (2014) 245–255.
[40] V. Jelenčić, M. Šestan, I. Kavazović, M. Lenartić, S. Marinović, T.D. Holmes, M. Prchal-Murphy, B. Lisnić, V. Sexl, Y.T. Bryceson, F.M. Wensveen, B. Polić, NK cell receptor NKG2D sets activation threshold for the NCR1 receptor early in NK cell development, Nat. Immunol. 19 (10) (2018) 1083–1092.
[41] B. Zafirova, F.M. Wensveen, M. Gulin, B. Polić, Regulation of immune cell function and differentiation by the NKG2D receptor, Cell. Mol. Life Sci.: CMLS 68 (21) (2011) 3519–3529.
[42] W. Chen, W. Lian, Y. Yuan, M. Li, The synergistic effects of oxaliplatin and piperlongumine on colorectal cancer are mediated by oxidative stress, Cell Death Dis. 10 (8) (2019) 600.
[43] M. Gagat, M. Hałas-Wiśniewska, W. Zielińska, M. Izdebska, D. Grzanka, A. Grzanka, The effect of piperlongumine on endothelial and lung adenocarcinoma cells with regulated expression of profilin-1, Onco Targets Ther. 11 (2018) 8275–8292.
[44] Z. Liu, Z. Shi, J. Lin, S. Zhao, M. Hao, J. Xu, Y. Li, Q. Zhao, L. Tao, A. Diao, Piperlongumine-induced nuclear translocation of the FOXO3A transcription factor triggers BIM-mediated Apoptosis in cancer cells, Biochem. Pharmacol. 163 (2019) 101–110.
[45] C. Zhang, L.-J. He, Y.-B. Zhu, Q.-Z. Fan, D.-D. Miao, S.-P. Zhang, W.-Y. Zhao, X.-P. Liu, Piperlongumine inhibits Akt phosphorylation to reverse resistance to cisplatin in human non-small cell lung cancer cells via ROS regulation, Front. Pharmacol. 10 (2019) 1178.
[46] P. Zhang, L. Shi, T. Zhang, L. Hong, W. He, P. Cao, X. Shen, P. Zheng, Y. Xia, P. Zou, Piperlongumine potentiates the antitumor efficacy of oxaliplatin through ROS induction in gastric cancer cells, Cell. Oncol. (Dordr.) 42 (6) (2019) 847–860.
[47] H. Wang, Y. Wang, H. Gao, B. Wang, L. Dou, Y. Li, Piperlongumine induces apoptosis and autophagy in leukemic cells through targeting the PI3K/Akt/mTOR and p38 signaling pathways, Oncol. Lett. 15 (2) (2018) 1423–1428.
[48] S.-S. Han, D.-J. Son, H. Yun, N.L. Kamberos, S. Janz, Piperlongumine inhibits proliferation and survival of Burkitt lymphoma in vitro, Leuk. Res. 37 (2) (2013) 146–154.
[49] K. Piska, P. Koczurkiewicz, D. Wnuk, E. Karnas, A. Bucki, K. Wójcik-Pszczoła, M. Jamrozik, M. Michalik, M. Kołaczkowski, E. Pękala, Synergistic anticancer activity of doxorubicin and piperlongumine on DU-145 prostate cancer cells - The involvement of carbonyl reductase 1 inhibition, Chem. Biol. Interact. 300 (2019) 40–48.
[50] G.Y. Liou, P. Storz, Reactive oxygen species in cancer, Free Radic. Res. 44 (5) (2010) 479–496.
[51] V. Aggarwal, H.S. Tuli, A. Varol, F. Thakral, M.B. Yerer, K. Sak, M. Varol, A. Jain, M.A. Khan, G. Sethi, Role of reactive oxygen species in cancer progression: molecular mechanisms and recent advancements, Biomolecules 9 (11) (2019).
[52] A.E. Li, H. Ito, I.I. Rovira, K.S. Kim, K. Takeda, Z.Y. Yu, V.J. Ferrans, T. Finkel, A role for reactive oxygen species in endothelial cell anoikis, Circ. Res. 85 (4) (1999) 304–310.
[53] C. Gorrini, I.S. Harris, T.W. Mak, Modulation of oxidative stress as an anticancer strategy, Nat. Rev. Drug Discovery 12 (12) (2013) 931–947.
[54] D. Trachootham, J. Alexandre, P. Huang, Targeting cancer cells by ROS-mediated mechanisms: a radical therapeutic approach? Nat. Rev. Drug Discovery 8 (7) (2009) 579–591.
[55] H. Möhler, R.W. Pfirrmann, K. Frei, Redox-directed cancer therapeutics: Taurolidine and Piperlongumine as broadly effective antineoplastic agents (review), Int. J. Oncol. 45 (4) (2014) 1329–1336.
[56] P. Zou, M. Chen, J. Ji, W. Chen, X. Chen, S. Ying, J. Zhang, Z. Zhang, Z. Liu, S. Yang, G. Liang, Auranofin induces Apoptosis by ROS-mediated ER stress and mitochondrial dysfunction and displayed synergistic lethality with piperlongumine in gastric cancer, Oncotarget 6 (34) (2015) 36505–36521.
[57] S.W. Ryter, S.M. Cloonan, A.M. Choi, Autophagy: a critical regulator of cellular metabolism and homeostasis, Mol. Cells 36 (1) (2013) 7–16.
[58] G. Kroemer, B. Levine, Autophagic cell death: the story of a misnomer, Nat. Rev. Mol. Cell Biol. 9 (12) (2008) 1004–1010.
[59] S. Chauhan, Z. Ahmed, S.B. Bradfute, J. Arko-Mensah, M.A. Mandell, S. Won Choi, T. Kimura, F. Blanchet, A. Waller, M.H. Mudd, S. Jiang, L. Sklar, G.S. Timmins, N. Maphis, K. Bhaskar, V. Piguet, V. Deretic, Pharmaceutical screen identifies novel target processes for activation of autophagy with a broad translational potential, Nat. Commun. 6 (2015) 8620.
[60] A.M. Jackson, A.B. Alexandroff, M.B. Lappin, K. Esuvaranathan, K. James, G. D. Chisholm, Control of leucocyte function-associated antigen-1-dependent cellular conjugation by divalent cations, Immunology 81 (1) (1994) 120–126.
[61] P.J. Neeson, P.J. Thurlow, G.P. Jamieson, Characterization of activated lymphocyte-tumor cell adhesion, J. Leukoc. Biol. 67 (6) (2000) 847–855.
[62] O.F. Ramos, M. Patarroyo, E. Yefenof, E. Klein, Requirement of leukocytic cell adhesion molecules (CD11a-c/CD18) in the enhanced NK lysis of iC3b-opsonized targets, J. Immunol. 142 (11) (1989) 4100–4104.
[63] T. Timonen, M. Patarroyo, C.G. Gahmberg, CD11a-c/CD18 and GP84 (LB-2) adhesion molecules on human large granular lymphocytes and their participation in natural killing, J. immunol. 141 (3) (1988) 1041–1046.
[64] M.S. Osman, D.N. Burshtyn, K.P. Kane, Activating Ly-49 receptors regulate LFA-1-mediated adhesion by NK cells, J. Immunol. 178 (3) (2007) 1261–1267.
[65] L. Monaco-Shawver, L. Schwartz, F. Tuluc, C.J. Guo, J.P. Lai, S.M. Gunnam, L. E. Kilpatrick, P.P. Banerjee, S.D. Douglas, J.S. Orange, Substance P inhibits natural killer cell cytotoxicity through the neurokinin-1 receptor, J. Leukoc. Biol. 89 (1) (2011) 113–125.
[66] X. Chen, D.S.J. Allan, K. Krzewski, B. Ge, H. Kopcow, J.L. Strominger, CD28-stimulated ERK2 phosphorylation is required for polarization of the microtubule organizing center and granules in YTS NK cells, Proc. Natl. Acad. Sci. U. S. A. 103 (27) (2006) 10346–10351.
[67] E.S. Sunila, G. Kuttan, Immunomodulatory and antitumor activity of Piper longum Linn. and piperine, J. Ethnopharmacol. 90 (2–3) (2004) 339–346.